Available online at www.sciencedirect.com
SCIENCE DIRECT
Electrochimica Acta 51 (2006) 2255–2260
ELECTROCHIMICA Acta
www.elsevier.com/locate/electacta

Application of atomic force microscopy and scaling analysis of images to predict the effect of current density, temperature and leveling agent on the morphology of electrolytically produced copper

T. Zhao, D. Zagidulin, G. Szymanski, J. Lipkowski *,[1]

Department of Chemistry, University of Guelph, Guelph, Ont., Canada N1G 2W1

Received 10 May 2005; received in revised form 31 May 2005; accepted 1 June 2005
Available online 12 September 2005

Dedicated to Professor Z. Galus on the occasion of his 70th birthday and in recognition of his contribution to electrochemistry.

Abstract

Atomic force microscopy (AFM) was used to study the morphology of electrodeposited Cu at current densities from 183 to 253 A m^{-2}. Digital image analysis was employed to parameterize the morphological information encoded in AFM images and to extract information concerning the mechanism of the electrodeposition reaction. It has been shown how the limiting roughness, δ, the critical scaling length, L_c and the aspect ratio, $4\delta/L_c$, vary as a function of the deposition time and electrodeposition conditions, such as temperature, current density and the amount of organic additives. It has been demonstrated how laboratory experiments of short duration and the scaling analysis of AFM images can be used to predict roughness of the metal sample after 2 weeks of industrial electrorefining.

Keywords: AFM; Surface roughness; Scaling analysis; Copper electrodeposition; Leveling

1. Introduction

Production of many metals, particularly, Ni, Cu, Zn, Ag and Au involves electrolytic methods based on the metal electrodeposition reaction. In the past, the metal electrodeposition reaction has been characterized chiefly in terms of current–voltage or current–time curves. Various models of the mechanism that describe nucleation and growth under various constraints, such as diffusion-limited, charge-transfer-limited and substrate-enhanced growth [1–3] have been proposed. However, these models cannot be used to explain and to predict surface morphology of electrodeposited material.

Spectacular advances in surface imaging techniques, such as atomic force microscopy (AFM) or white light interference microscopy (WLIM) have introduced new tools for the study of the morphology of electrodeposited metal. The scaling analysis of these images allows one to characterize the growth of the deposited metal in terms of its surface roughness and periodicity of surface features in the direction parallel to the surface (grain sizes). Monitoring evolution of these parameters as a function of the deposition time allows one to predict the morphology of industrially produced metal with the help of a laboratory experiment of a relatively short duration [4]. The scaling analysis has been successfully applied to describe deposition of copper in the presence of organic additives [5,6], deposition of gold and platinum [7], thin films of tin on steel [8] and electrorefining of nickel [9].

The parameters derived from the scaling analysis also provide an insight into surface growth mechanisms. Herring [10] proposed that the surface roughness results from a random material deposition (stochastic roughness), which is opposed by lateral smoothing processes [4,11–15], such as; dissolution and re-deposition, surface diffusion and volume diffusion.

* Corresponding author.
E-mail address: jlipkows@uoguelph.ca (J. Lipkowski).
[1] ISE member.

0013-4686/$ – see front matter © 2005 Elsevier Ltd. All rights reserved.
doi:10.1016/j.electacta.2005.06.042

The objective of this paper is to illustrate the power of AFM imaging combined with scaling analysis to predict the morphology of copper electrodeposited at conditions mimicking industrial copper electrorefining. We will also show how to use this technique to optimize the electrorefining parameters, such as the current density, temperature and concentration of organic additives. Modern AFM instruments allow imaging of a surface area that is 150 μm × 150 μm wide and the height of the imaged objects may not exceed 6 μm. This imposes restrictions on the duration of the electrolysis, which as a rule should not exceed 10 h. The deposition time of the industrially produced copper is on the order of 10 days and the roughness is usually in excess of 10 μm. The roughness of industrial samples can be measured with the help of WLIM. We will demonstrate that the AFM images acquired for a laboratory sample corresponding to 10 min of electrodeposition can be scaled up to predict the surface morphology after 100 h of electrodeposition (4 days). The scaled up AFM images will be compared to WLIM images of industrial copper produced after 4 days of electrodeposition. We will show an excellent agreement between the roughness and morphology displayed by the scaled up image of a laboratory sample and the image of the industrial sample. We will provide conclusive evidence that the morphological and topological information obtained by AFM imaging of copper produced in a laboratory experiment of a relatively short duration is relevant for industrial production of copper. Preliminary results of this work were presented in Ref. [16].

2. Experimental

2.1. Electrodeposition

Copper electrodeposition was carried out using a two-electrode electrochemical cell consisting of counter (CE) and working (WE) electrodes. The current density was controlled by a galvanostat (VersaStat, EG&G Potentiostat/Galvanostat). The cathode was a 6 mm diameter copper slug embedded in resin. It was hand-polished with 600, 800 and then 1200 grade SiC paper, followed by polishing at a cloth containing 1 μm alumina powder. The electrode was then cleaned in an ultra-sonic cleaner to remove alumina, for a period of 10 min. The polished electrode was placed in a methanol solution for degreasing.

The electrochemical cell is shown schematically in Fig. 1. Two hundred milliliters of an industrial electrolyte was circulated between the electrochemical cell and the reservoir, maintained at the desired operating temperature. A typical elemental composition of the electrolyte in g/L was; 40 Cu; 22 Ni; 152 H_2SO_4; 5.5 Na; 2.5 As; 0.2 Bi. The volume ratio between the cell and the reservoir was about 1:2.5. To mimic the industrial hydrodynamic regime, the flow rate of the electrolyte (measured as volume/time) was equal to the rate used in copper electrorefining, scaled down

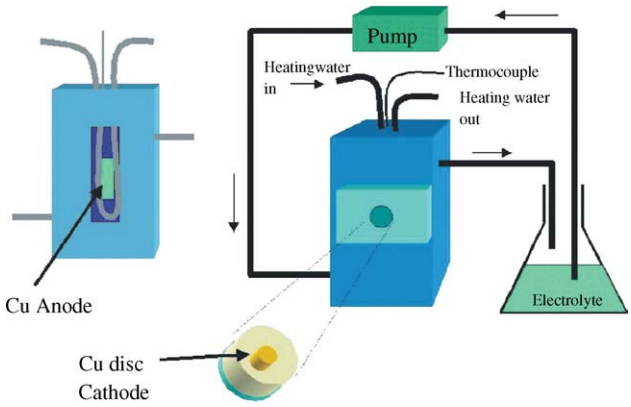

Fig. 1. Diagram of the electrochemical cell.

using the ratio of the volume of the industrial tank to the volume of the experimental cell.

After each deposition, the cathode was rinsed with deionized water. The surface was then imaged by AFM using different scan sizes. For each plating condition, samples of electrodeposited metals were collected for a series of electrodeposition times. Morphology of the electrodeposited copper was investigated at; (i) 54.5, 65 and 76.7 °C using current density 183 A m^{-2} and (ii) for 213 and 253 A m^{-2} at 65 °C. Glue and tembind (commercial names of a mixture of organic compounds) were used as leveling agents.

AFM images were captured using Nanoscope E AFM (Digital Instruments, CA) using silicon nitride tips (Digital Instruments) which had a nominal spring constant of 0.06 N/m. All images were acquired in height mode, with both gains ∼3, at scan rates between 7 and 12 Hz. No filtering of images was performed other then inherent in the feedback loop.

The White Light Interference Microscope, model WYKO NT3300 (Veeco Metrology, Tucson, Arizona) was used to capture images of the industrial samples using different magnifications (5, 10, 27, 51 and 104).

3. Results

Figs. 2 and 3 depict the principles of the method. Fig. 2 shows a series of AFM images of the surface of copper acquired after various deposition times, using 183 A m^{-2}, temperature 65 °C and with addition to 6 mg/L of glue and 250 mg/L of tembind. This constitutes the standard condition of electrorefining and will be referred to as the standard condition.

In order to extract the morphological information, the scaling analysis was performed on every image. Fig. 3 illustrates the principle of the scaling analysis. In the scaling analysis the image is divided into a grid of squares with the side length (scaling length) L. One calculates the root-mean-square of the surface heights (rms) or the standard deviation of the surface heights within each square and then averages this standard

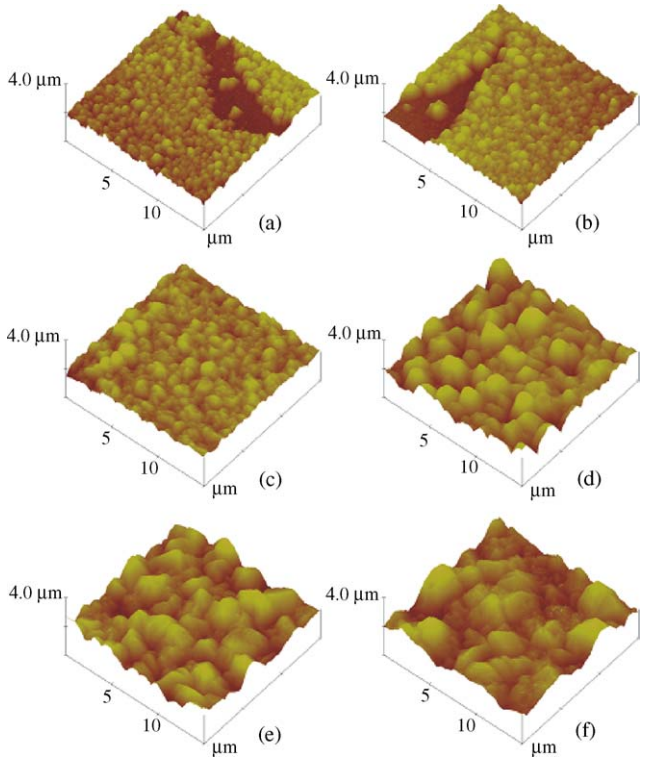

Fig. 2. AFM images of electrodeposited copper from the solution with 6 mg/L of glue and 250 mg/L of tembind at 183 A m^{-2} and at 65 °C for the following deposition times: (a) 0.5 min, (b) 1 min, (c) 2 min, (d) 3 min, (e) 5 min and (f) 10 min.

deviation over all squares to determine (ξ_L) defined as [4,12]:

$$\xi_L = \sqrt{\langle [H(x, y) - \langle H(x, y)\rangle]\rangle^2}. \quad (1)$$

The calculation is repeated using another grid of squares with a different value of the scaling length L and then ξ_L is plotted versus L in logarithmic coordinates. In Eq. (1), $H(x,y)$ is the height at the point x,y at the surface, measured with respect to an arbitrary reference plane.

Fig. 3 shows the $\log \xi_L$ versus $\log L$ plots for four samples corresponding to different deposition times. For larger values of the length scale L, the parameter ξ_L attains a limiting roughness (δ). The presence of a plateau at the $\log \xi_L$ versus $\log L$ plots indicates that for a sufficiently large L the measured roughness parameter becomes independent of the scaling length. The scaling theory predicts that the time dependence of the limiting roughness, is described by:

$$\delta \propto t^{\beta} \quad (2)$$

where β is the growth exponent. The growth exponent may be easily determined from the slope of the $\log \delta$ versus $\log t$ plot.

At lower values of the length scale, $\log \xi_L$ varies in a linear fashion as a function of $\log L$. In fact, the scaling theory predicts that in this range:

$$\xi_L \propto L^{\alpha} \quad (3)$$

where α is the static exponent and its value should be independent of the electrolysis time. The magnitude of parameter α reveals the dominant mechanism of the surface growth. The static exponent is related to the coefficient $n = 2(\alpha + 1)$, that can be independently determined from the spectral power density analysis of the images (Fourier transform analysis of the image). The parameter $n = 4$ indicates that the deposition is controlled by surface diffusion while $n = 3$ indicates that the smoothing of the surface is due to the so called volume flow which can be identified as the progressive nucleation mechanism.

The characteristic length L at which the surface roughness attains the limiting value is called the critical scaling length (L_c). The critical scaling length measures periodicity of surface features in the direction parallel to the surface.

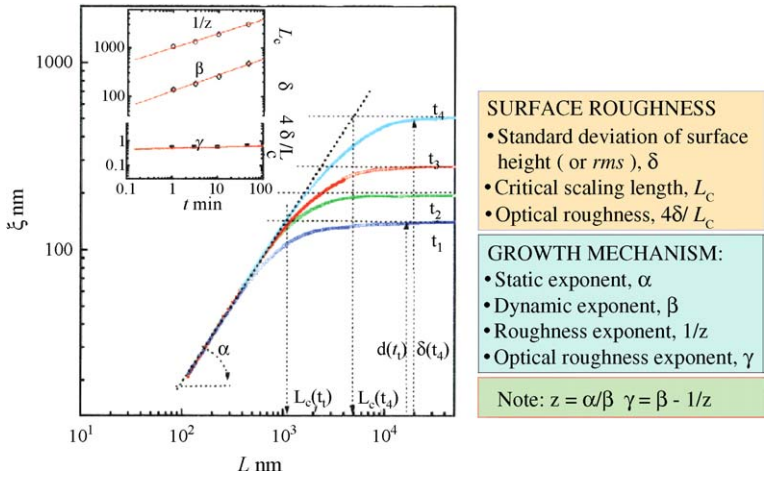

Fig. 3. Representative plot of the standard deviation of the surface height, ξ_L as a function of the scale length for several growth times. The plateau in the ξ_L vs. L curves defines the root mean square (rms) limiting roughness δ. The scale length L corresponding to the knee in the curves is the critical scaling length, L_c. Both δ and L_c increase with the deposition time. The inset shows standard log–log plot of L_c, δ and $4\delta/L_c$ vs. time used to determine the roughness exponent $1/z$, the dynamic exponent β and the aspect ratio (optical roughness) exponent γ.

Table 1
Values of the scaling analysis parameters describing the morphology of electrodeposited copper at investigated conditions

Experimental variable	Condition	$4\delta/L_c\ ct^{\gamma}$ (μm)	$\delta\ at^{\beta}$ (μm)	$L_c\ bt^{1/z}$ (μm)	α	n
Temperature (& 183 A m^{-2} and 6 mg/L glue)	54.5 °C	$0.42t^{-0.03}$	$0.097t^{0.35}$	$0.959t^{0.38}$	0.78	4.0
	65.0 °C	$0.61t^{-0.05}$	$0.130t^{0.34}$	$0.869t^{0.40}$	0.80	3.9
	76.7 °C	$0.59t^{-0.13}$	$0.152t^{0.35}$	$1.030t^{0.44}$	0.66	3.9
Current density (& 65.0 °C)	213 A m^{-2}	$0.34t^{0.03}$	$0.088t^{0.40}$	$1.031t^{0.36}$	0.73	3.7
	253 A m^{-2}	$0.51t^{0.01}$	$0.108t^{0.40}$	$0.869t^{0.40}$	0.77	4.1
Glue concentration (& 183 A m^{-2} and 65 °C)	3 mg/L	$0.52t^{-0.03}$	$0.139t^{0.31}$	$1.090t^{0.34}$	0.78	3.9
	9 mg/L	$0.56t^{-0.11}$	$0.118t^{0.35}$	$0.829t^{0.44}$	0.73	3.9

The theory predicts that L_c depends on time according to the scaling law:

$$L_c \propto t^{1/z} \tag{4}$$

where $1/z$ is the roughness exponent. The ratio of $4\delta/L_c$ is the aspect ratio that is a measure of the ratio of the height to the width of a periodic feature on a corrugated surface (for example, ratio of the grain height to the grain width). The dependence of the aspect ratio on time is described by:

$$\frac{4\delta}{L_c} \propto t^{\gamma} \tag{5}$$

where γ is the optical roughness exponent. The time dependence of δ, L_c and $4\delta/L_c$ is shown in the inset to Fig. 3. The advantage of the scaling analysis is that the mechanism of growth and the evolution of the surface morphology with the electrodeposition time may be described in terms of four exponents α, β, $1/z$ and γ. The exponent α provides information concerning the mechanism of surface growth, while exponents: β, $1/z$ and γ show how the height, width and the aspect ratio of surface features change with the deposition time. The values of parameters determined from the scaling analysis are reported in Table 1.

Fig. 4a shows scaling analysis performed on WLIM images of industrial samples. Sample A corresponds to copper produced after 16 days and sample C after 16 h of electrorefining. The scaling analysis of copper produced in the laboratory at conditions mimicking industrial electrorefining but using deposition times shorter than 10 min are shown in the left bottom corner of Fig. 4a. The results show that the laboratory and industrial samples scale according to the same law. Fig. 4b plots the limiting roughness as a function of the deposition time. The points corresponding to the industrial samples are lying on the line plotted through the points determined from the scaling analysis of the AFM images. This is an important result as it shows that a laboratory experiment can be used to predict the surface roughness of copper produced in a refinery.

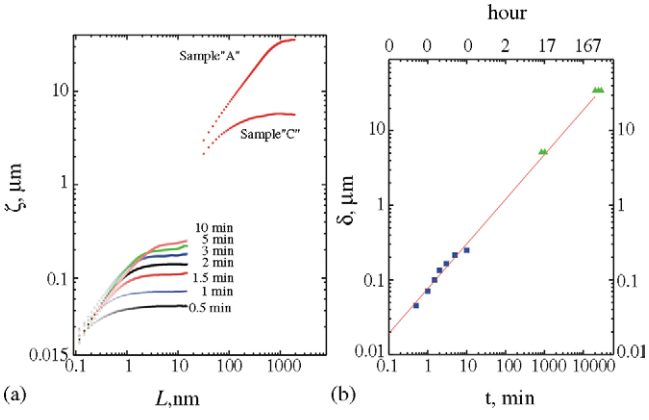

Fig. 4. (a) Scaling analysis of two industrial samples "A" and "C" images (sample "A" deposition time ~16 days, sample "C" deposition time 16 h) using WLIM and seven laboratory samples images using AFM. (b) Plot of the limiting roughness vs. time determined from the scaling analysis of images.

The scaling parameters determined from AFM images can be used to rescale an image of electrodeposited copper produced in a short duration laboratory experiment to predict the morphology of the metal after 10 days of electrorefining. Fig. 5a shows an image of a predicted surface morphology of copper after 10 days of electrorefining obtained by rescaling an image of a laboratory sample corresponding to 45 min of electrodeposition. For comparison Fig. 5b is a WLIM image of an industrial sample after 10 h of electrorefining. The two images show similar size grains that are actually sharper and better resolved in the image scaled up from an AFM experiment.

The lateral resolution of the WLIM is determined by the diffraction of light limit and is on the order of ~1 μm. The resolution of an AFM image is determined by the image size divided by the number of pixels and is better than ~0.2 μm. This is why more features could be seen in the scaled up AFM image. Taking the differences between the lateral resolution of the two techniques into account, the similarity between the predicted and the actual image of the industrial sample is remarkable. This example illustrates the power of AFM and scaling analysis to predict morphological changes in the electrolytically produced copper as a function of various electrodeposition conditions.

The second level of image analysis involves calculation of the autocovariance function (ACF) [17–20]. The ACF is the product of two exact copies of the image when they are shifted relative to each other by a separation r. The ACF of a rough surface is defined by [4]:

$$G(|r|) = \langle h(r_j)h(r_i)\rangle - \langle h(r)\rangle^2 \tag{6}$$

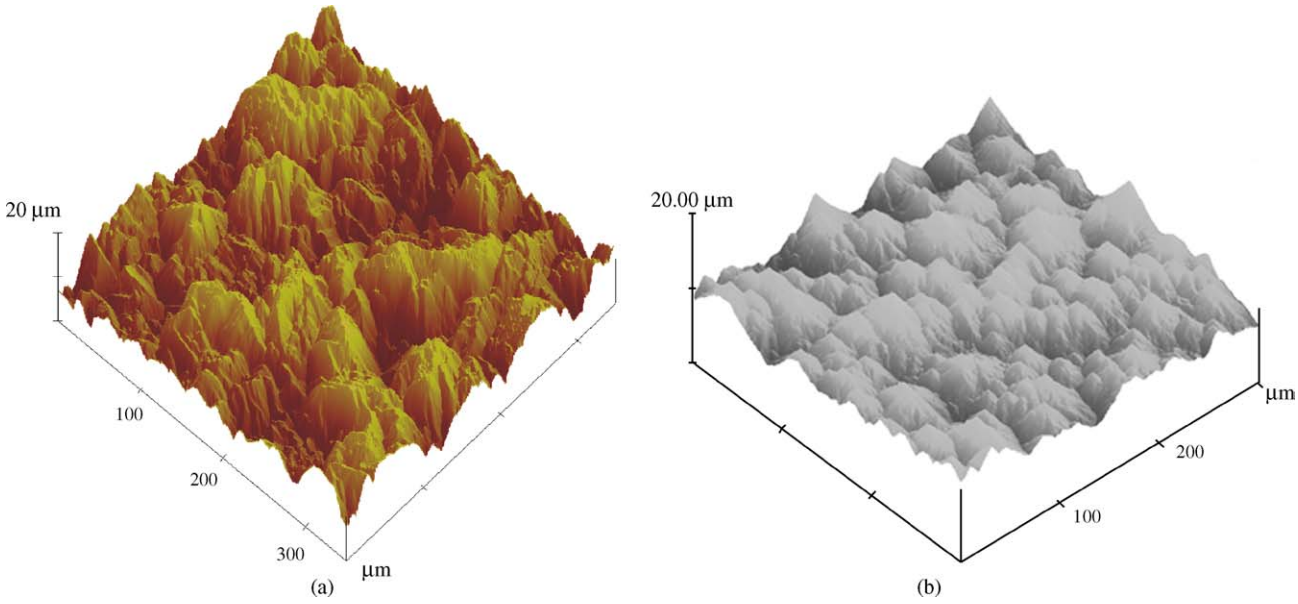

Fig. 5. (a) Predicted surface topology of copper produced by 10 days of electrodeposition by scaling up an AFM image of a sample obtained after 10 min of deposition in our laboratory; (b) WLIM image of copper surface produced after 10 days of electrorefining in a copper electrorefinery. Both samples were produced by electrodeposition from the standard electrolyte solution at 183 A m^{-2} and 65 °C.

where $r = |r_j - r_i|$ is the separation or lag length. Fig. 6 shows representative ACF calculated for one image from Fig. 2. The function $G(|r|)$ probes the correlation between features on a rough surface as a function of their separation distance, with nonzero values indicating correlated structures. The value of ACF at the origin of coordinates is equal to variance δ^2, hence the limiting surface roughness is equal to: $\delta = \sqrt{G(|r = 0|)}$. The value of r at which the ACF crosses zero for the first time is the critical scaling length L_c. It is related to the correlation length (σ) by the formula; $\sigma = L_c\sqrt{\alpha}/\pi$ [4].

The Fourier transform of the ACF gives the spectral power density or structure factor for the rough surface [21]:

$$g(|q|) \equiv \Im[G(|r|)] \tag{7}$$

where $\Im$ is the two-dimensional Fourier transform operator and q is the wave number. Fig. 7 plots the spectral power density (SPD) calculated from the ACF shown in Fig. 6. At low frequencies the SPD attains a limiting value related to the limiting surface roughness by $\alpha\delta^2 L_c^2/\pi$. At high frequencies the SPD decreases linearly with $\log q$. The slope of this plot is equal to the exponent n which provides useful information concerning the smoothing mechanism. The value of $n = 1$ is observed when smoothing is due to the viscous flow of an amorphous material; $n = 2$ for smoothing resulting from the dissolution and re-deposition, $n = 3$ for the bulk diffusion or the progressive nucleation, finally $n = 4$ when smoothing is caused by the surface diffusion. The slope of the plot in Fig. 7 is ~4 and this indicates that the smoothing mechanism involves surface diffusion. While the calculation of ACF provides essentially the same morphological information as the scaling analysis, the SPD determined from the Fourier transformation of ACF provides valuable insight into the origin of the smoothing mechanism.

The AFM imaging and the two levels of digital image analysis were employed to study the effect of various electrorefining conditions, such as variable temperature, variable current density and variable glue concentration on the morphology of electrodeposited copper. The range of these parameters was relatively narrow. However, it was

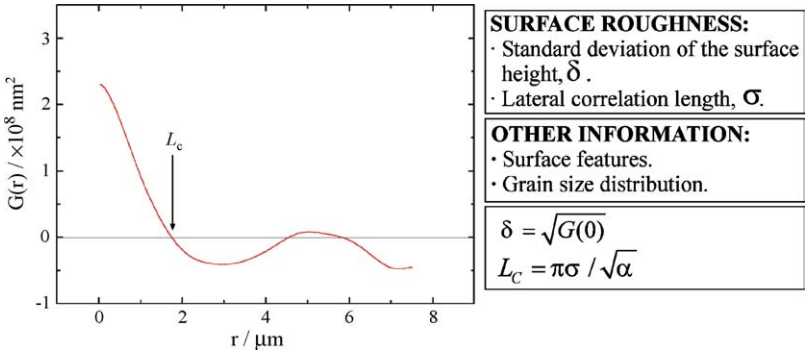

Fig. 6. Representative example of the ACF calculated from the image (e) in Fig. 2.

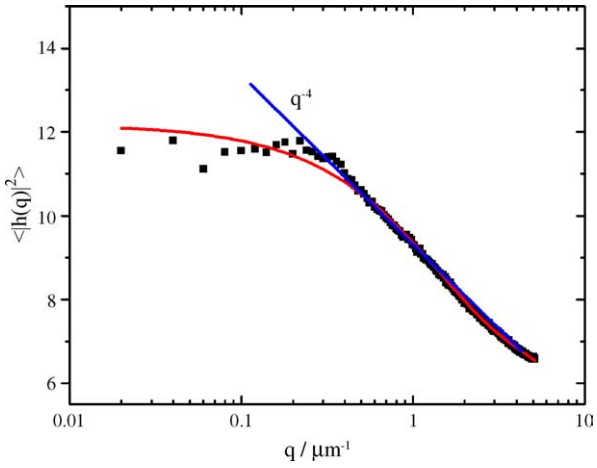

Fig. 7. Representative example of the SPD calculated from the ACF in Fig. 6. Predominant smoothing mechanism: viscous flow ($n = 1$), evaporation and condensation ($n = 2$), bulk diffusion ($n = 3$) and surface diffusion ($n = 4$).

typical for a change that may take place during industrial copper electrorefining. Table 1 describes the morphology of copper, electrodeposited at these experimental conditions, in terms of parameters determined from the scaling analysis of the AFM images. Columns one and two describe the experimental condition. Columns three to five report values of the surface roughness, the critical length and the aspect ratio at any value of deposition time. These numbers may be used to calculate the surface roughness and the width of the surface features (grains) at a desired time of the electrorefining.

The last two columns in Table 1 report the values of the static scaling coefficient α and the smoothing coefficient n. We recall that according to the theory $n = 2(\alpha + 1)$. The values of n determined from the SPD were approximately equal to 4 under all the experimental conditions. The values of n calculated from α were on the order of 3.5. These numbers indicate that surface diffusion was the predominant smoothing mechanism [4].

The following predictions can be made with the help of parameters listed in Table 1. The surface roughness and the critical length increase with temperature. However, the roughness increases faster with time than the critical length. At a longer electrolysis time, the aspect ratio of grains in copper produced at 76.7° will be smaller than at 54.5°. The surface produced at the highest temperature will be more leveled and the deposit will consist of larger grains. There is surprisingly little effect of the current density on the morphology of electrodeposited copper. Parameters β, $1/z$ and γ change little with the current density. In addition γ is close to zero indicating that the aspect ratio changes very little with the deposition time. The experiments carried out using solutions with glue concentrations of 3, 6 and 9 mg/L show that the surface roughness decreases but the critical scaling length increases when more glue is present in the electrolyte. This causes a significant decrease of the aspect ratio. Clearly, glue acts as a typical leveling agent. Copper with a smoother and more leveled surface is produced when the glue content in the electrolyte increases.

4. Summary and conclusions

Atomic force microscopy has been shown to be a powerful tool for studying surface morphologies of electrodeposited metals. The digital image analysis allows one to encode the morphological information contained in the image of electrodeposited metal in the magnitude of a few numerical parameters. These parameters may then be used to predict the surface morphology of a metal produced by prolonged electrolysis, from an experiment of short duration.

We have applied this method to investigate the effect of temperature, current density and glue concentration on the morphology of electrodeposited copper. A relatively narrow range of these parameters, typical for a change that may take place during copper electrorefining, were investigated. The results of these experiments may help the refinery to either optimize the electrolytic production of copper or to predict the effect of an unexpected change of the electrodeposition conditions.

References

[1] E. Bosco, S.K. Rangarajan, J. Electroanal. Chem. 134 (1982) 213.
[2] J.O'M. Bockris, G.A. Razumny, Fundamental Aspects of Electrocrystallization, Plenum Press, NY, 1967.
[3] B. Scharifker, G. Hills, Electrochim. Acta 28 (1983) 879.
[4] W.M. Tong, R.S. Williams, Annu. Rev. Phys. Chem. 45 (1994) 401.
[5] W.U. Schmidt, R.C. Alkire, A.A. Gewirth, J. Electrochem. Soc. 143 (1996) 3122.
[6] H. Iwasaki, T. Yoshinobu, Phys. Rev. B 48 (1993) 8282.
[7] J.M. Gomez-Rodriguez, A.M. Baro, L. Vazquez, R.C. Salvarezza, J.M. Vara, J. Phys. Chem. 96 (1992) 347.
[8] T. Jiang, N. Hall, A. Ho, S. Morin, Thin Solid Films 471 (2005) 76–85.
[9] G. Szymanski, M. Pogoda, B. Campbell, J. Lipkowski, Proceedings of the 27th Annual Hydrometallurgical Meeting of CIM Nickel–Cobalt, Sudbury, 1997.
[10] C. Herring, J. Appl. Phys. 21 (1950) 301.
[11] D.D. Vvedensky, A. Zangwill, C.N. Luse, M.R. Wilby, Phys. Rev. E 48 (1993) 852.
[12] A.-L. Barabasi, H.E. Stanley, Fractal Concepts in Surface Growth, Cambridge University Press, New York, 1995.
[13] E.A. Eklund, E.J. Synder, R.S. Williams, Surf. Sci. 285 (1993) 157.
[14] D.G. Stearns, Appl. Phys. Lett. 62 (1993) 1745.
[15] G. Palasantzas, J. Krim, Phys. Rev. Lett. 73 (1994) 3564.
[16] G. Szymanski, M. Dymarska, T. Zhao, J. Lipkowski, Proceedings of the 31st Annual Hydrometallurgy Meeting, Canadian Institute of Mining, Metallurgy and Petroleum (CIM), Toronto, Ont., Canada, August 26–29, 2001, p. 375.
[17] H. Iwasaki, T. Yoshinobu, Phys. Rev. B 48 (1993) 8282.
[18] G. Kahanda, X. Zou, R. Farre, P. Wong, Phys. Rev. Lett. 68 (1992) 3741.
[19] D.P. Barkey, R.H. Muller, C. Tobias, J. Electrochem. Soc. 136 (1989) 2199.
[20] P. Garic, D. Barkey, E.B. Jacob, E. Bochner, N. Broxholm, B. Miller, B. Orr, R. Zamir, Phys. Rev. Lett. 69 (1989) 2703.
[21] J.M. Elson, H.E. Bennett, J.M. Bennett, in: R.R. Shannon, J.C. Wyant (Eds.), Applied Optics and Optical Engineering, vol. 8, 1979, p. 191.